# Quasiperiodic instabilities and their exchange of criticality with harmonic and subharmonic modes in temperature-modulated Rayleigh-Benard convection

Mehdi Riahi [1,2,*] and Mohamed Hayani Choujaa[3]
[1]*Department of Mechanics, Royal Air School, Marrakech, Morocco*
[2]*Mohammed V University in Rabat, Mohammadia School of Engineers, ERG2(ME), Av. Ibn Sina, Rabat, Morocco*
[3]*Laboratory of Mechanics, Faculty of Sciences Aïn Chock, University Hassan II, B.P 5366, Mâarif, Casablanca, Morocco*

(Received 7 February 2026; accepted 7 August 2026; published 24 August 2026)

Previous studies dealing with Floquet stability analysis of non-zero-mean time-modulated Rayleigh-Bénard convection have shown the existence of only harmonic and subharmonic instability modes. Here, we emphasize the existence of quasiperiodic instabilities that have not yet been reported in the literature. This is achieved through both a Floquet-based analysis of the basic state and direct numerical simulations of the linearized stability equations. Particular attention is devoted to highlighting the existence of kinks in the numerically computed marginal stability curves that render difficult the detection of the stability exchange between quasiperiodic instabilities and their harmonic and subharmonic counterparts. Depending on the Prandtl number of the working fluid, such instability exchanges set in via either bicritical states or the migration of complex-conjugate pairs Floquet multipliers which can be combined to produce subharmonic responses.

DOI: 10.1103/zfs5-hwlt

## I. INTRODUCTION

Despite the substantial body of work devoted to the stability of thermally modulated convection, existing studies have almost exclusively focused on the occurrence of two types of instabilities where the disturbances, at the instability onset, are either synchronous with the periodic forcing or subharmonic, having half the forcing frequency [1–5]. In particular, the stability landscape has been systematically interpreted within this restricted framework, implicitly assuming the absence of more complex temporal responses. Consequently, the possible occurrence of quasiperiodic instabilities, associated with incommensurate temporal scales and complex Floquet spectra, has remained largely unexplored. This lack of attention constitutes a significant gap in the current literature, especially for the classic system of Rayleigh-Bénard convection, where a horizontal Newtonian fluid layer with infinite extent is subjected to a time-dependent temperature at the boundaries.

Motivated by the recently reported quasiperiodic instabilities in time-modulated convection in a horizontal Hele-Shaw cell by Riahi *et al.* [6,7], we aim, in the present paper, to shed light on their existence in horizontal cells with infinite extent. This is the case where the basic state loses stability via a Neimark-Sacker bifurcation, as dictated by the Floquet theory. Such quasiperiodic states are encountered in many time-periodically forced systems including time-modulated Taylor-Coutte flow [8–11], periodically driven cavity flows [12,13], and thermal convection under gravitational modulation [14]. A quasiperiodic solution means that the system's response is no longer directly and solely dependent on the frequency forcing but becomes dependent on a new frequency called the "Neimark-Sacker frequency." It is interesting to emphasize here that the appearance of quasiperiodic instability modes is a direct consequence of the parametric excitation of the system.

The occurrence of quasiperiodic states is not foreign to classical (unmodulated) Rayleigh-Bénard convection, where they have been reported as a result of secondary bifurcations and nonlinear mode interactions arising beyond the primary stationary instability. In the present case, however, the mechanism is fundamentally different. The periodically varying control parameter introduces an external forcing frequency into the system. The resulting Floquet problem permits resonant interactions between the forcing and the perturbation dynamics, leading to parametric resonance, and under appropriate conditions, to quasiperiodic instability modes characterized by two incommensurate frequencies.

Floquet theory is one of the powerful tools that has been widely used to investigate transitions in time-periodically forced systems whose dynamics are generally governed by partial differential equations. Two different approaches regarding the implementation of Floquet theory are encountered in the literature depending on how space and time behaviors are treated.

In the first approach, Galerkin's method is employed to describe the spatial behavior of the system by expanding it onto a truncated series of orthogonal polynomials. This reduces the governing equations to a finite set of ordinary differential equations having generally the form of Hill or Mathieu equations [1,15]. The time-dependent amplitudes of

*Contact author: mehdi_riahi@hotmail.fr

*Published by the American Physical Society under the terms of the Creative Commons Attribution 4.0 International license. Further distribution of this work must maintain attribution to the author(s) and the published article's title, journal citation, and DOI.*

the spatial modes are subsequently analyzed in the sense of Floquet, suggesting that a general solution $\phi(t)$ may be written as

$$\phi(t) = \phi_b(t) + e^{\mu t} X(t), \tag{1}$$

with $\phi_b(t)$ the periodic solution corresponding to the basic state about which the Floquet analysis is performed and $X(t)$ generally a time-dependent function called also the Floquet mode, which is also periodic with period $T_f = 2\pi/\omega$ where $\omega$ denotes the dimensionless frequency forcing. The complex quantity $\mu = \mu_r + \mu_i$ is referred to as the characteristic Floquet exponent whose real part $\mu_r$ determines the growth rate of the disturbance while its imaginary part $\mu_i$ is a second frequency associated with quasiperiodic motion of the system. The quantity $\lambda = e^{2\pi\mu/\omega}$ defines the corresponding Floquet multiplier. A generalization of Eq. (1) consists of expanding $X(t)$ into a truncated complex Fourier series in time

$$X(t) = \sum_{p=-\infty}^{+\infty} X_p e^{ip\omega t}. \tag{2}$$

For $t = T_f$, we have $e^{ip\omega T_f} = e^{i2\pi p} = 1$ and so Eq. (1) becomes

$$\phi(T_f) = \phi_b(T_f) + e^{2\pi\mu_r/\omega} e^{i2\pi\mu_i/\omega} \sum_{p=-\infty}^{+\infty} X_p. \tag{3}$$

The modulus and argument of the Floquet multiplier are given respectively by $|\lambda| = e^{2\pi\mu_r/\omega}$ and $\arg(\lambda) = 2\pi\mu_i/\omega$. Substituting the expression (2) into the time-dependent first order stability equations leads ultimately to a homogeneous algebraic system that exhibits a necessary and sufficient condition for the existence of nontrivial solutions by vanishing of its characteristic determinant which defines a dispersion relation relating all the parameters of the problem.

A slightly different implementation of this numerical procedure has been widely used in the literature where the time dependence is treated before the spatial one. In this case, the partial differential equations are transformed into an infinite space-dependent system using expressions (1) and (2). The existence of nontrivial solutions is conditioned on the vanishing of the corresponding characteristic determinant. This numerical approach has been employed by Seminara and Hall [16] when studying the stability of a Stokes layer around a circular cylinder oscillating in an infinite fluid and adopted in numerous studies [11,13,17] dealing with Floquet analysis of well-defined time-periodic basic states. Marginal stability curves are computed by imposing $\mu_r = 0$ while harmonic and subharmonic responses are sought by imposing $\mu_i = 0$ and $\mu_i/\omega = 1/2$, respectively. In this context, quasiperiodic responses could not be readily identified as they require the determination of the exact value of $\mu_i$ for which the associated determinant vanishes. This is one of the disadvantages of this numerical procedure that does not give sufficient importance to quasiperiodic solutions corresponding generally to $\mu_i \neq 0$.

The second approach is different in the sense that it is based on Floquet multiplier calculations instead of expanding the physical variables in terms of the truncated Fourier series. Such a Floquet analysis is considered more rigorous and robust because it does not impose values to the Floquet exponent but instead calculates it, or, equivalently, its associated Floquet multiplier. The latter represent the calculated eigenvalues of the so-called Monodromy matrix stemming from a spatial discretization of the stability equations followed by a numerical integration over one forcing period.

In this paper, this second approach is adopted to revisit the linear stability of time-modulated Rayleigh-Bénard convection. The main purpose is to shed light on the existence of Neimark-Sacker bifurcations corresponding to quasiperiodic instability modes that have not yet been reported in the literature.

## II. MATHEMATICAL FORMULATION AND NUMERICAL SET UP

Consider a Newtonian fluid layer of kinematic viscosity $\nu$ and thermal diffusivity $\kappa$, confined between two infinite horizontal rigid planes and subjected to time-periodic thermal boundary conditions with a nonzero mean temperature difference. The temperatures of the lower and upper planes are defined respectively as $T^*(z^* = 0) = T_1^* = T_h + T_m \cos(\omega^* t^* + \phi)$ and $T^*(z^* = d) = T_2^* = T_c + \delta T_m \cos(\omega^* t^*)$ (with $T_h \succ T_c$). Here, $d$, $z^*$, $t^*$, $T_m$, and $\omega^*$ denote, respectively, the distance between the horizontal planes, vertical coordinate, time, modulation amplitude, and modulation frequency, while $\delta$ stands for the modulation amplitude ratio between the upper and lower boundaries. The parameter $\phi$ represents the phase-lag of the thermal modulation.

The quantities $d^2/\kappa$, $d$, and $T_h - T_c$ are used as time, space, and temperature scales, respectively. The dimensionless temperature field $T$ is related to the dimensional temperature field $T^*$ by $T = (T^* - T_c)/(T_h - T_c)$. The instantaneous temperature difference across the layer is given by

$$\Delta T(t) = \overbrace{1}^{\text{steady component}} + \varepsilon \overbrace{[\cos(\omega t + \phi) - \delta\cos(\omega t)]}^{\text{oscillatory component}}, \tag{4}$$

with $\varepsilon = T_m/(T_h - T_c)$ and $\omega$ the dimensionless frequency number defined by $\omega = \omega^* d^2/\kappa$.

The temperature profile in the quiescent base state corresponds to a pure conductive regime, written as a superposition of a steady component (generated by the steady temperature gradient at the boundaries) and an oscillatory thermal-Stokes component (induced by the time-periodic forcing), measured by the parameter $\varepsilon$. It is given by

$$T^0(z,t) = \overbrace{1 - z}^{\text{steady component}} + \varepsilon \overbrace{\text{Re}[f(z,t)]}^{\text{oscillatory component}}. \tag{5}$$

The superscript "0" denotes the base temperature profile and Re indicates the real part of the function $f$ given by

$$f(z,t) = \frac{\sinh(\sqrt{i\omega}(1-z))e^{i\phi} + \delta\sinh(\sqrt{i\omega}z)}{\sinh\sqrt{i\omega}} e^{i\omega t}. \tag{6}$$

Following Yih and Li [1], a linear stability analysis is then performed which consists in superimposing infinitesimal perturbations on this basic state. In the context of the Boussinesq approximation and after eliminating the pressure and horizontal velocities, we obtain the following linearized perturbation

equations:

$$\mathrm{Pr}^{-1}\nabla^2\frac{\partial w}{\partial t} = \nabla^4 w - \mathrm{Ra}\nabla_\perp^2\hat{T},$$
$$\frac{\partial \hat{T}}{\partial t} = \nabla^2\hat{T} + \frac{\partial T^0}{\partial z}\tilde{w}, \tag{7}$$

with $w(x, y, z, t)$ and $\hat{T}(x, y, z, t)$ the infinitesimal perturbations of the vertical velocity and the temperature field, respectively. The horizontal Laplacian $\nabla_\perp^2$ is defined as $\partial^2/\partial x^2 + \partial^2/\partial y^2$, with $x$ and $y$ being the horizontal streamwise and spanwise directions, respectively. The behavior of this perturbed system is controlled by the frequency number $\omega$, the Rayleigh number $\mathrm{Ra} = \frac{\beta g(T_h - T_c)d^3}{\nu\kappa}$ and the Prandtl number $\mathrm{Pr} = \nu/\kappa$ where $\beta$ is the thermal expansion coefficient of the fluid. We further assume the perturbations are periodic along the horizontal directions

$$w(x, y, z, t) = \tilde{w}(z, t)e^{i(K_1 x + K_2 y)}, \tag{8}$$

$$\hat{T}(x, y, z, t) = \tilde{T}(z, t)e^{i(K_1 x + K_2 y)}, \tag{9}$$

where $K_1$ and $K_2$ denote, respectively, the wave numbers in the streamwise and spanwise directions. By substituting the expressions (8) and (9) into the stability system (7), the following linear partial differential equations governing the linear dynamics of the system are obtained:

$$\left(M - \mathrm{Pr}^{-1}\frac{\partial}{\partial t}\right)M\tilde{w} = K^2\mathrm{Ra}\tilde{T},$$
$$\left(M - \frac{\partial}{\partial t}\right)\tilde{T} = \frac{\partial T^0}{\partial z}\tilde{w}, \tag{10}$$

associated with the boundary conditions

$$\tilde{w}(0) = \tilde{w}(1) = \frac{\partial\tilde{w}(0)}{\partial z} = \frac{\partial\tilde{w}(1)}{\partial z} = \tilde{T}(0) = \tilde{T}(1) = 0. \tag{11}$$

Here, $M = \frac{\partial^2}{\partial z^2} - K^2$ where $K = \sqrt{K_1^2 + K_2^2}$ is the wave number of the convective cells. The quantities $(\tilde{w}, \tilde{T})(z, t)$ represent, respectively, the amplitudes of the $z$-direction velocity and temperature perturbations. It should be emphasized here that since the basic state is homogeneous and isotropic in the horizontal plane, the linear stability equations are invariant under horizontal rotations. Consequently, the eigenvalue problem depends only on the magnitude of the horizontal wave vector $K$ and not on its orientation.

### A. Floquet-based analysis

Since the linear stability problem is governed by a system of time-dependent partial differential equations (written in detail in Refs. [1–3]), we combine Floquet theory with a spectral method based on the Chebyshev-Gauss-Lobatto scheme using $N$ collocation points defined in the interval $[-1, 1]$. This procedure leads to a spatially discretized system of ordinary differential equations involving $(2N)$ time-dependent unknowns, which can be written in the Floquet form

$$\overline{\overline{\mathrm{B}}}\frac{\partial}{\partial t}\widehat{\mathbf{X}} = \overline{\overline{\mathbf{M}}}(t)\widehat{\mathbf{X}} = [\mathbf{M}_0 + \mathbf{M}_c\cos(\omega t) + \mathbf{M}_s\sin(\omega t)]\widehat{\mathbf{X}}, \tag{12}$$

where $\widehat{\mathbf{X}}$ is the state vector containing the expansion coefficients of the velocity and temperature perturbations. The matrix $\overline{\overline{\mathbf{M}}}(t)$ is a $2\pi/\omega$ periodic whereas $\overline{\overline{\mathbf{B}}}$, $\mathbf{M}_0$, $\mathbf{M}_c$, and $\mathbf{M}_s$ are constant coefficient matrices. Integrating over a forcing period $T_f = 2\pi/\omega$, using a fourth-order Runge-Kutta numerical scheme, we obtain the monodromy matrix of the system whose eigenvalues $\lambda_j$, called Floquet multipliers, control the growth rate of the perturbations and determine the nature of the bifurcated solution depending on its critical value. More details about this numerical approach could be found in Refs. [18–21]. It is to be noted that our numerical code is validated through comparisons with a variety of similar flow configurations including time-modulated thermal convection about zero-mean [2,3] and narrow-gap time-modulated Taylor-Couette flow [17,20,22–24].

We recall here that, for the assigned values to the parameters $K$, Ra, Pr, $\omega$, $\varepsilon$, $\delta$, and $\phi$, we aim to address a marginal stability curve separating unstable and stable regimes. Indeed, based on the modulus $|\lambda_j|$, stability of the basic state is ensured as long as $|\lambda_j| \prec 1$ for all calculated eigenvalues, whereas instability is reached when at least one multiplier satisfies $|\lambda_j| \succ 1$. At the instability onset, there exists at least one eigenvalue that lies on the unit circle, i.e., $|\lambda_j| = 1$. In this case, harmonic and subharmonic responses correspond respectively to $(\lambda_r, \lambda_i) = (1, 0)$ and $(\lambda_r, \lambda_i) = (-1, 0)$ where $(\lambda_r, \lambda_i)$ denote the real and imaginary parts of the unstable eigenvalue, respectively. However, when dealing with quasiperiodic responses a pair of complex-conjugate eigenvalues, e.g., $\lambda_1 = \lambda_r + i\lambda_i$ and $\lambda_2 = \lambda_r - i\lambda_i$, crosses the unit circle such that $|\lambda_1| = |\lambda_2| = 1$ [18,19,26,27].

### B. Direct numerical simulations

To further assess the reliability of the Floquet-based approach as well as the corresponding in-house numerical code, the partial differential equations governing the linear stability of the systems (10) and (11) are resolved using another numerical procedure that does not rely on eigenvalue computations. This procedure consists of a direct numerical simulation (DNS) based on the classical finite-difference method, using centered approximations for the spatial derivatives and an implicit scheme for the temporal integration. Using suitable initial conditions together with temporal and spatial steps of order $10^{-3}$, the stability of the system is determined on the basis of the time series of the perturbations.

Marginal stability curves are constructed by assigning the values of $K$, Pr, $\varepsilon$, $\delta$, $\phi$, and $\omega$ and then looking for the critical Rayleigh number at which the perturbations neither grow nor decay. An example is shown in Fig. 1, which shows the time series of the vertical velocity perturbation at $(x, y, z) = (0, 0, 1/2)$ over 25 modulation periods for $K = 3.8$, $\mathrm{Pr} = 7$, $\varepsilon = 3.3$, $\delta = 1$, $\phi = 0$, and $\omega = 51.82$.

The system becomes unstable at $\sqrt{\mathrm{Ra}_c} = 49.1$ meaning that for $\sqrt{\mathrm{Ra}_c} \succ 49.1$ this perturbation amplitude grows [see Fig. 1(c)] and decays for $\sqrt{\mathrm{Ra}_c} \prec 49.1$ [see Fig. 1(a)]. The nature of the bifurcated solution could also be identified from this time evolution. Indeed, subharmonic and harmonic responses are characterized by periods $4\pi/\omega$ and $2\pi/\omega$, respectively. Thus, over 25 forcing periods, a subharmonic response exhibits only for 12.5 oscillation cycles, whereas

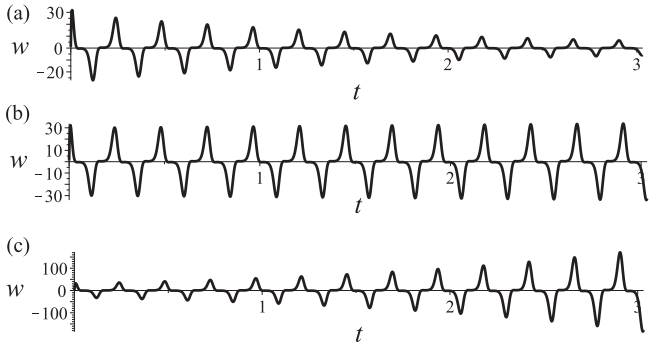



FIG. 1. Evolution over 25 periods of the vertical velocity component of the perturbation field stemmed from DNS and recorded at $(x, y, z) = (0, 0, 1/2)$ and different values of Rayleigh number when $\varepsilon = 3.3$, $\omega = 51.82$, $\phi = 0$, $K = 3.8$, and $\mathrm{Pr} = 7$. (a) $\mathrm{Ra}^{1/2} = 49.1 \prec \mathrm{Ra}_c^{1/2}$, (b) $\mathrm{Ra}_c^{1/2} = 49.82$, (c) $\mathrm{Ra}^{1/2} = 50 \succ \mathrm{Ra}_c^{1/2}$.

a harmonic response exhibits 25 cycles. It is, consequently, quite clear that the solution displayed in Fig. 1 corresponds to a subharmonic response.

A comparison between the Floquet analysis and DNS is illustrated in Fig. 2 showing examples of the marginal stability curves for two representative cases, namely, $(\varepsilon, \omega) = (3.3, 51.82)$ and $(\varepsilon, \omega) = (10, 40.5)$. An excellent agreement between the two approaches is clearly remarked. Such an agreement provides reliability to our Floquet analysis, which will therefore be adopted throughout the remainder of the investigation.

## III. RESULTS

In Fig. 3, we illustrate the marginal stability curves showing the evolution of Rayleigh number versus wave number $K$ at the frequency $\omega = 162$ and $\mathrm{Pr} = 7$ where the parameter $\varepsilon$ varies between 0 and 40.

As one can see, we recover at $\varepsilon = 0$ the marginal stability curve of the unmodulated case where instability is reached

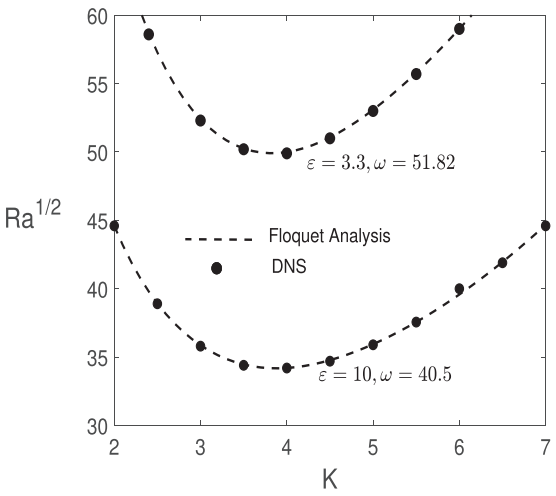



FIG. 2. Marginal stability curve showing comparison between Floquet analysis and direct numerical simulation results for the cases $(\varepsilon = 10\ \omega = 40.5)$ and $(\varepsilon = 3.3\ \omega = 51.82)$ when $\phi = 0$, $\delta = 1$, and $\mathrm{Pr} = 7$.

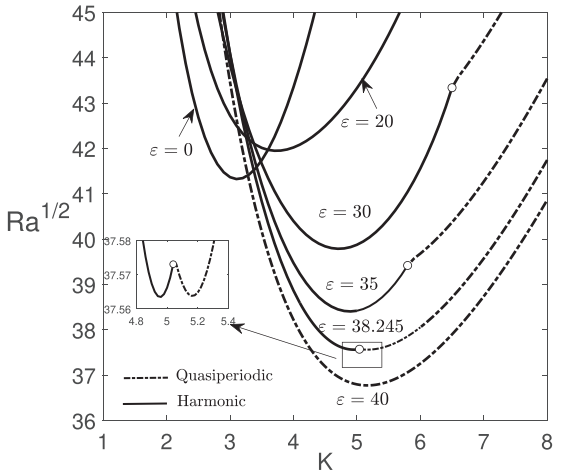



FIG. 3. Marginal stability curves showing the emergence of quasiperiodic states for different values of the parameter $\varepsilon$ at $\omega = 162$, $\delta = 1$ and $\phi = 0$ for $\mathrm{Pr} = 7$.

at $\mathrm{Ra}_c^{1/2} = 41.31$ and $K_c = 3.1$. A weakly stabilizing effect is observed by increasing the modulation amplitude up to $\varepsilon = 20$ where the obtained numerical critical instability parameters are $\mathrm{Ra}_c^{1/2} = 41.95$ and $K_c = 3.7$. This instability mode is mainly driven by the steady component of the thermal boundary conditions, i.e., given in Eq. (4), and consequently it represents a parametric excitation of the classical steady Rayleigh-Bénard mode where the convective cells are rotating in a privileged direction of rotation despite the presence of oscillatory thermal gradient. In this case, and owing to the large value of the modulation frequency $\omega$, the thermal modulation does not considerably alter the instability onset since, as it is commonly known, the oscillatory component of the basic state generates thermal waves confined in narrow regions near the horizontal walls called "thermal Stokes layer" and here we are dealing with the thermal skin phenomenon. This feature is no longer conserved by greatly increasing $\varepsilon$ which measures the intensity of the oscillatory thermal drive. As one can notice, a destabilizing effect of the thermal modulation is observed when $\varepsilon \succ 20$, as indicated by the downward shift of these neutral stability curves, accompanied by the existence of a kink separating harmonic and quasiperiodic solutions. This kink shifts toward the low-wave number regime under an increase in the parameter $\varepsilon$ and eventually disappears at $\varepsilon = 40$. The primary bifurcation remains harmonic and mainly driven by the steady component of the thermal drive as long as $\varepsilon \prec 38.245$ and a bicritical state between harmonic and quasiperiodic instability modes is reached at $\varepsilon = 38.245$. This is a codimension-two bifurcation point where the system exhibits two coexisting solutions characterized by the same critical Rayleigh number and two incommensurate wave numbers. When $\varepsilon \succ 38.245$, we are dealing with only quasiperiodic solutions emerging in the form of parametric resonances predominantly driven by the oscillatory component of the thermal drive. It is interesting to point out that the detection of such bicriticality becomes possible only after a zoom in the Rayleigh number axis is performed where $\mathrm{Ra} \in [37.56, 37.58]$, i.e., a width of only 0.02 in Rayleigh number units.

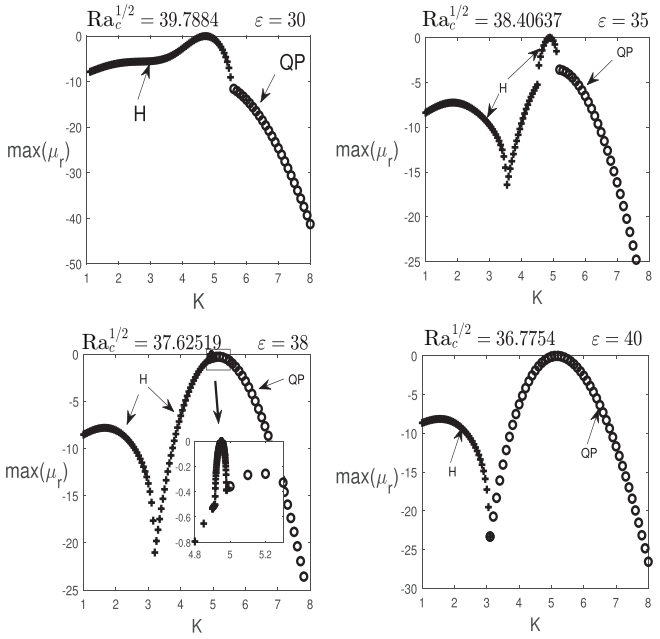



FIG. 4. Growth rate of the perturbations computed at the critical Raymeigh number for $\omega = 162$, $\mathrm{Pr} = 7$ and different values of $\varepsilon$. The continuous lines represent harmonic solutions while quasiperiodic ones are represented by dashed-dot lines.

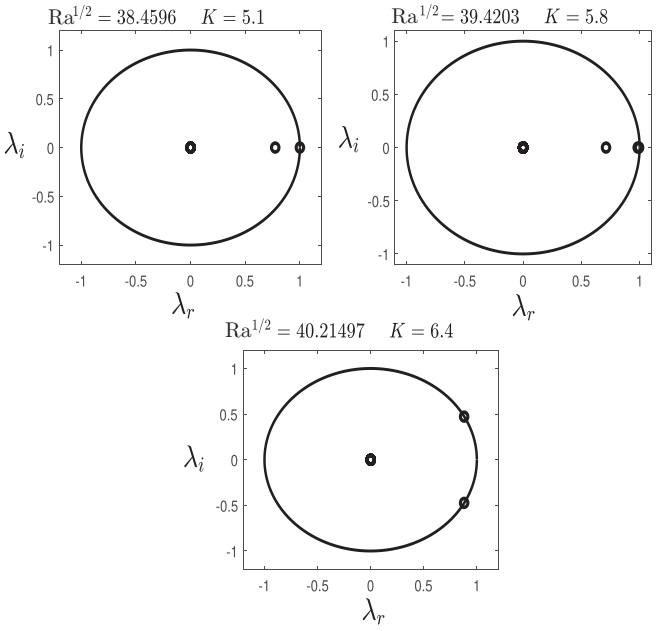



FIG. 5. Floquet multipliers showing the nature of some stability points presented at $\varepsilon = 35$ in Fig. 3. Parameters are chosen as in the Fig. 3.

Detecting such bicriticality experimentally is challenging because it looks like a single bifurcation point unless specifically sought with high-resolution techniques. The instability exchange between two instability modes with different nature is usually obvious from numerically computed marginal stability curves that are generally composed by tongue-like curves. Examples include the instability exchange between harmonic reversing and nonreversing flows in time-modulated Taylor-Couette flow [20,23,25] and between harmonic and subharmonic modes in thermal convection subjected to different time-periodic forcing [6,14]. This is to mention that in some forced hydrodynamical systems, changes in the nature of the primary bifurcation could not be easily visible unless the marginal stability curves are adequately examined. The presence of kinks, i.e., points of nondifferentiability, in these curves could be a signature of such instability exchange. In what follows, the term kink refers to a point of nondifferentiability at which the left- and right-hand derivatives are finite but unequal.

It should be emphasized that this neutral curve was numerically continued well beyond the displayed wave-number interval. This continuation reveals that the observed structure is not a simple intersection of two loop-like marginal branches, but rather a kink-like feature of the stability boundary.

To remedy to this problem, one should have recourse to a visualization of the growth rate of the perturbations at different values of the Rayleigh number. This growth rate corresponds to the maximal value of the real part of Floquet exponent related to the Floquet multiplier through $\mu = \ln(\lambda)/T$. We report in Fig. 4 the evolution of the maximal values of $\mu_r$ versus the wave number under a gradual increase of $\varepsilon$ and at its corresponding critical Rayleigh number. As one can see, when $\varepsilon = 30$ a clear kink point is observed at $K = 5.8$ separating the two branches representing harmonic (left-hand) and quasiperiodic (right-hand) solutions. In this case, the quasiperiodic mode is still stable as long as its corresponding values of $\mu_r$ remain strictly negative because the chosen value of the Rayleigh number corresponds to that given by the marginal stability curve for the harmonic mode, i.e., $\mathrm{Ra}_c^{1/2} = 39.7884$. The instability synchronously sets in with the thermal drive at $K_c = 4.6$ as dictated by the marginal curve in Fig. 3. By gradually increasing $\varepsilon$, the maximal values of $\mu_r$ associated with the quaisperiodic mode increase and approach zero and it represents the most unstable mode at $\varepsilon = 40$ where $K_c = 5.2$ in agreement with the marginal curve.

To identify the nature of the different branches of the obtained marginal stability curves, we present, for instance, in Fig. 5 Floquet multipliers at $\varepsilon = 35$, for different values of the wave number $K$, and at the corresponding Rayleigh numbers. This figure considers the same parameter space as in Fig. 3 where the kink point is located at the wave number $K = 5.8$. As one can notice, at $K = 5.1$ and $K = 5.8$ we are dealing with harmonic solutions since all eigenvalues of the system are inside the Floquet circle except one eigenvalue that crosses the unit circle with $(\lambda_r, \lambda_i) = (1, 0)$. The solution is thus harmonic as are all points in the left-hand branch where $K \preceq 5.8$. However, at $K = 6.4$ a pair of complex-conjugate Floquet multipliers crosses the unit circle, i.e., $\lambda_{1,2} = \lambda_r \pm \lambda_i = 0.88154 \pm 0.47213i$ with $|\lambda_{1,2}| = 1$. This means that the right-hand side branch in the marginal stability curve corresponds to a quasiperiodic state where the basic state loses stability via a Neimark-Sacker bifurcation.

Since these quasiperiodic instabilities are detected only in the in-phase modulation case, a natural question can be raised regarding their occurrence by varying the parameters $\phi$ and $\delta$ because at $\phi = 180^\circ$ (or equivalently $\delta = -1$) and $\delta = 0$ no quasiperiodic modes are found. For this purpose,

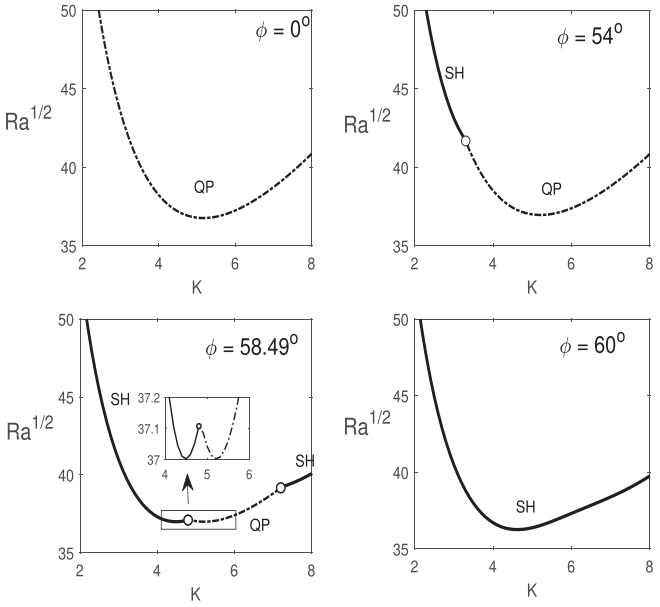



FIG. 6. Marginal stability curves showing progressive germination-like phenomenon of subharmonic solutions under a gradual increase of the parameter $\phi$ when $\omega = 162$, Pr = 7, and $\varepsilon = 40$.

we illustrate in Fig. 6 the marginal stability curves at $\omega = 162$, $\delta = 1$, Pr = 7, $\varepsilon = 40$, and different values of $\phi$. As one can notice, a subharmonic instability branch appears at $\phi = 54^\circ$ separated from the quasiperiodic instability branch by a kink point at $K \approx 3.3$. Increasing $\phi$ beyond this value, a "germination-like" process of the subharmonic modes is observed from the left and the right sides of the quasiperiodic branch in the sense that the latter becomes bounded between two subharmonic branches fed continuously by the increase of the parameter $\phi$. A codimension-two bifurcation point is reached at $\phi = 58.49$ where the quasiperiodic and the subharmonic modes emerge simultaneously with two incommensurate wave numbers. Such a bifurcation point becomes discernible only after zooming in on the Rayleigh number scale. The quasiperiodic mode is totally suppressed at $\phi = 60^\circ$. It is important to point out that these quasiperiodic and subharmonic modes are parametric resonances since they are computed at a high value of $\varepsilon$, i.e., $\varepsilon = 40$.

The transition between these instabilities occurs in a smooth way by varying the parameter $\delta$ as it is depicted in Fig. 7 illustrating the marginal stability curves at $\omega = 162$, $\phi = 0$, Pr = 7, $\varepsilon = 40$, and different values of $\delta$. Two distinct tongue-like marginal stability curves are computed representing quasiperiodic and subharmonic instabilities. The quasiperiodic nature of the primary bifurcation is preserved up to $\delta = 0.552$ where a codimension-two bifurcation point is reached and beyond which only suharmonic solutions exist similarly to the case when he thermal modulation concerns only the lower plate, i.e., $\delta = 0$.

A different behavior is observed by changing the physical properties of the working fluid especially the kinematic viscosity and thermal diffusivity whose ratio is given by the Prandtl number. By choosing air as a fluid with low Prandtl number, i.e., Pr = 0.71, quasiperiodic instabilities are also

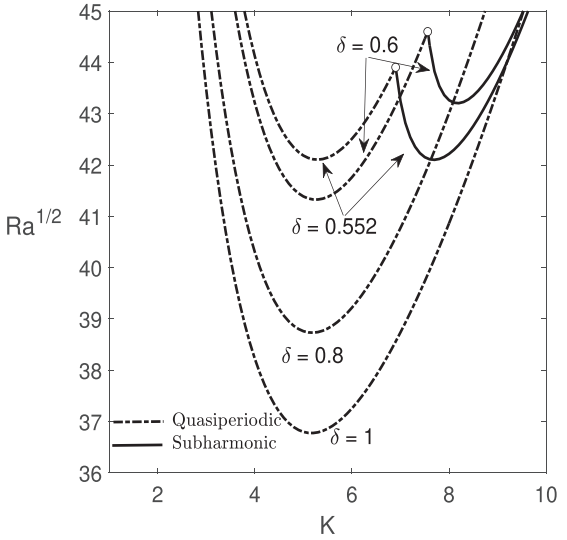



FIG. 7. Marginal stability curves showing the emergence of the first bicritical state when the parameter $\delta$ increases at $\omega = 162$, Pr = 7, $\phi = 0$, and $\varepsilon = 40$.

detected for the same thermal boundary conditions considered in Fig. 3 for Pr = 7. The primary bifurcation remains harmonic up to $\varepsilon = 16.4$ where a codimension-two bifurcation point is detected. In this case, quasipepriodic instabilities appear at $\varepsilon = 10$, but represent the most unstable mode when $\varepsilon \succ 16.4$. These features are illustrated in the marginal stability curves depicted in Fig. 8. The system in this parameter space does not exhibit subharmonic solutions.

By varying the parameter $\phi$ specifically at $\phi = 166^\circ$, this codimension-two bifurcation sets in at $\varepsilon = 13.69$ instead of $\varepsilon = 16.4$ when $\phi = 0^\circ$. This feature is clearly shown from the marginal stability curves depicted in Fig. 9.

As one can see, in addition, at the instability threshold, harmonic and quasiperiodic instability modes with different wave

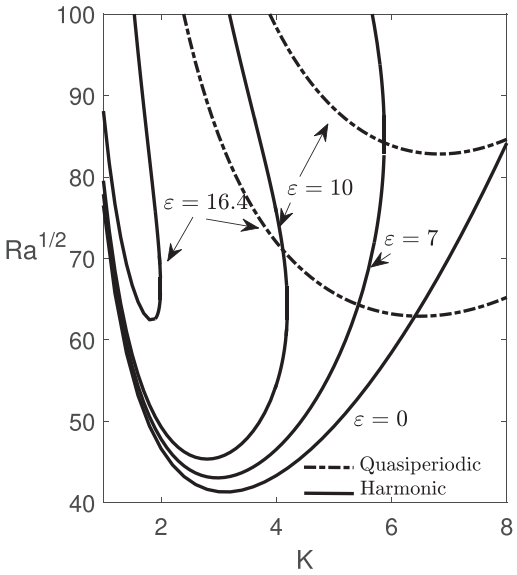



FIG. 8. Marginal stability curves showing the emergence of the first bicritical state when the parameter $\varepsilon$ increases at $\omega = 162$, $\phi = 0$, $\delta = 1$, Pr = 0.71.

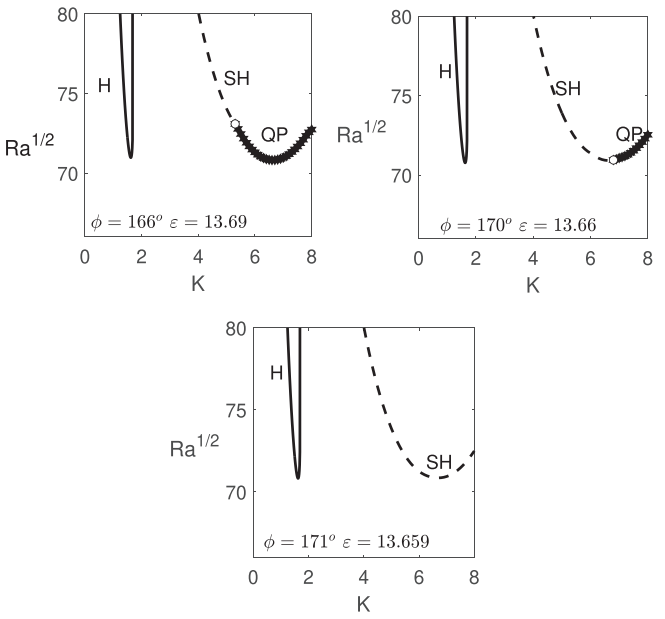



FIG. 9. Marginal stability curves showing the germination-like phenomenon of suharmonic solutions at bicriticality when $\omega = 162$, $\mathrm{Pr} = 0.71$, and $\delta = 1$.

number coexist. It is interesting to mention here the existence of a subharmonic branch undergoing a "germination-like" process when $\phi$ increases. This means that the parameter $\phi$ feeds subharmonic instabilities detrimental to the quasiperiodic instabilities that are totally suppressed at $\phi = 171^\circ$. This behavior could be explained by the fact that when $\phi$ approaches $180^\circ$, the temperatures at the lower and upper plates tend towards the out-phase case, characterized exclusively by subharmonic responses. The numerical values of the critical instability parameters computed at the bicritical states detected under a gradual variation of the parameters $\phi$ for $\omega = 162$ and $\delta = 1$ are given in Table I.

To get more insights into this dynamics, the Floquet multipliers are plotted in the complex plan in Fig. 10 at the instability onset. As one can remark, when $\phi = 30^\circ$, one purely real eigenvalue, computed at $K_c = 1.8$, crosses the Floquet circle along with a pair complex-conjugate eigenvalue computed at $K_c = 6.5$. By gradually increasing $\phi$, the complex

TABLE I. Numerical values of the critical instability parameters computed at the bicritical states detected under a gradual variation of the parameters $\phi$ for $\omega = 162$ and $\delta = 1$.

| $\phi$ | $\varepsilon$ | $K_c^S$ | $K_c^H$ | $K_c^{QP}$ | $\sqrt{\mathrm{Ra}_c}$ |
|---|---|---|---|---|---|
| 10 | 16.4 | – | 1.8 | 6.5 | 63.297 |
| 30 | 16.1 | – | 1.8 | 6.5 | 63.226 |
| 100 | 14.69 | – | 1.7 | 6.6 | 67.942 |
| 130 | 14.05 | – | 1.65 | 6.6 | 69.569 |
| 140 | 13.94 | – | 1.65 | 6.6 | 69.961 |
| 160 | 13.72 | – | 1.6 | 6.6 | 70.709 |
| 170 | 13.66 | – | 1.63 | 6.6 | 70.772 |
| 171 | 13.659 | 6.7 | 1.62 | – | 70.826 |

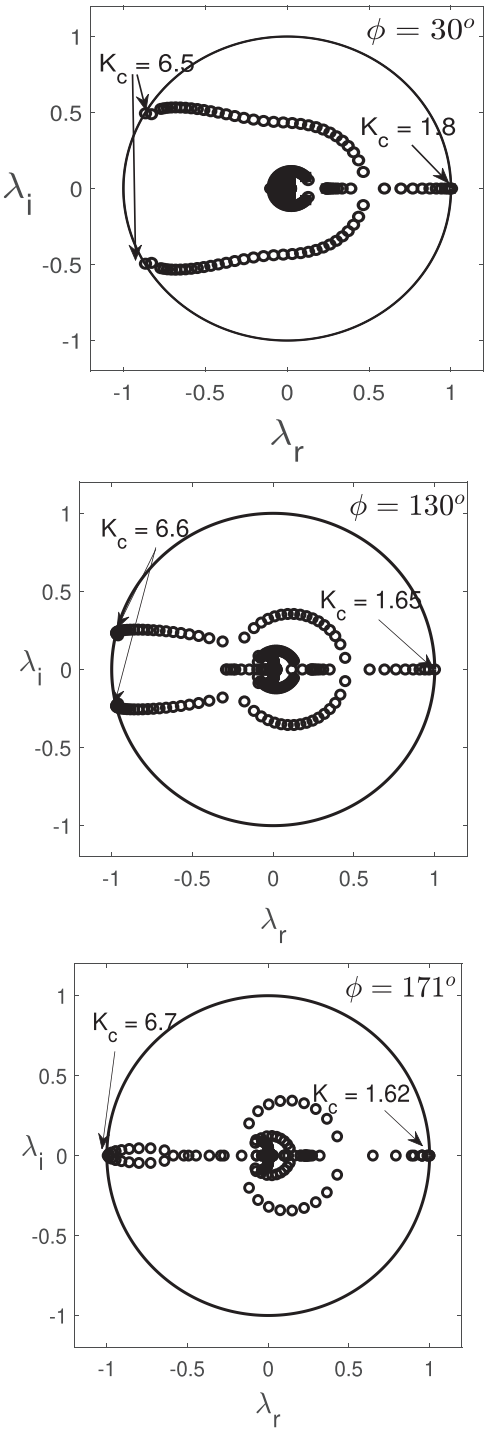



FIG. 10. Floquet multipliers with variations in the phase-lag parameter $\phi$ at $\omega = 162$, $\mathrm{Pr} = 0.71$, and $\delta = 1$ illustrating the evolution of a quasiperiodic mode having a pair of complex conjugate multiplier into a subharmonic mode having a purely negative multiplier.

eigenvalues migrate continuously to the real axis and merge to produce a subharmonic multiplier at $\phi = 171^\circ$.

## IV. COMPARISON AND DISCUSSION

Recently, Riahi *et al.* [6] studied the stability of the time-modulated Rayleigh-Bénard convection of a Newtonian fluid

confined in a horizontal Hele-Shaw cell under the same thermal boundary conditions as those considered in the present study. We recall here that with a Hele-Shaw cell, only the infinite extent in the streamwise direction is preserved while the spanwise direction becomes finite by inserting two vertical adiabatic plates of width $d$ separated by a distance $e$. The latter is supposed to be sufficiently small compared with the height of the geometry, i.e., $\epsilon \ll 1$ with $\epsilon = e/d$. As demonstrated by previous studies [15], the time-periodic forcing in Hele-Shaw cell alters the dynamics of the convective rolls only in the limit where $\mathrm{Pr} = O(\epsilon^2)$. This means that thermal parametric resonances are expected only for low Prandtl number fluids corresponding to liquid metals such as mercury, in contrast to the classic Rayleigh-Bénard cell where parametric resonances are present for all Prandtl number fluids. This is the first major difference between time-modulated Rayleigh-Bénard convection in a Hele-Shaw cell and that in a classic cell where the horizontal layer is laterally unconfined in both horizontal directions. However, these flow configurations exhibit numerous interesting similarities. The first one concerns the absence of quasiperiodic instabilities for low modulation frequencies as well as for single-plate and out-of-phase sinusoidal forcing at arbitrary frequency. The second one concerns the occurrence of quasiperiodic instabilities only in the in-phase forcing case at high frequencies. Indeed, for $\phi = 0$ and $\delta = 1$, the first bicritical state between harmonic and quasiperiodic modes occurs at $\varepsilon = 21.78$ in the Hele-Shaw cell instead of $\varepsilon = 16.4$ in the current study. The third similarity concerns the migration of the complex-conjugate Floquet multipliers and their merge into one real multiplier crossing the Floquet circle at $-1$ when the parameter $\phi$ increases. Such a phenomenon sets in at $\phi = 139.5^\circ$ in the Hele-Shaw case instead of $\phi = 171^\circ$ in the current study. This agreement suggests that the emergence of quasiperiodic modes is a robust feature of thermally modulated convection, irrespective of whether the flow is confined in a Hele-Shaw cell or evolves in a fully extended Rayleigh-Bénard layer.

It is to be noted that the replacement of quasiperiodic instability modes with subharmonic modes concerns also the dynamics of the wake of a square cylinder as reported by Sheard *et al.* [28] at a specified value of the angle of incidence. Such a transition is interpreted by Blackburn and sheard [29] as a result of a $Z_2$ spatiotemporal symmetry breaking of the wakes of the square cylinder when it is weakly rotated about its axis.

The occurrence of quasiperiodic instability modes concerns also the case of zero-mean time-modulated Rayleigh-Bénard system in Hele-Shaw cells as numerically demonstrated by Riahi *et al.* [7] in the in-phase modulation case. These authors showed that the primary bifurcated solution from the basic state remains quasiperiodic as long as the modulation frequency $\omega \succ 30.2$. Otherwise, the primary bifurcation becomes harmonic and the exchange between these bifurcations sets in through a codimension-two bifurcation point at $\omega = 30.2$. In contrast to the present study, no kink-mediated exchange of criticality between competing instabilities of different natures has been reported.

It is important to mention that quasiperiodic instability modes have been also encountered in other thermal convective systems undergoing gravitational forcing. One may cite, for instance, what was demonstrated by Chen and Chen [14] who investigated the effect of gravity modulation on the stability characteristics of convection in an infinite slot with two kinds of fluids, in particular, $\mathrm{Pr} = 1$ and $\mathrm{Pr} = 25$. Quasiperiodic modes are observed only in the case of $\mathrm{Pr} = 25$ with a modulation amplitude ratio of 0.5. This mode consists of two waves of different oscillation frequencies whose sum equals the forcing frequency and the oscillation frequency of the critical state under steady gravity. The case of horizontal double-diffusive fluid layers with cross-diffusion was investigated by Terrones and Chen [30] including rigid boundaries. For low Prandtl number ($10^{-2}$) double-diffusive fluid layers, these authors shed light on the existence of bifurcating neutral curves with double minima, one of which corresponds to a quasiperiodic branch while the other to a subharmonic solution.

## V. CONCLUSION

In this investigation, we demonstrated, using a Floquet-based stability analysis supported by direct numerical simulations, that a time-periodic thermal forcing can give rise to genuinely quasiperiodic instabilities in Rayleigh-Bénard convective systems in addition to the previously reported harmonic and subharmonic modes. The occurrence of these quasiperiodic instabilities is associated with kink-like features in the marginal stability curves, which can obscure stability exchanges and likely give explanation of their absence in earlier studies. The transition from these quasiperiodic modes to subharmonic modes sets in via either the migration of complex-conjugate Floquet multipliers or bicritical states in the marginal stability curves. These results highlight the importance of computing Floquet exponents without *a priori* assumptions and reveal an additional layer of dynamical complexity in thermally modulated convection.

## DATA AVAILABILITY

The data and numerical tools that support the findings of this study are available from the authors upon reasonable request.

[1] C. S. Yih and C. H. Li, Instability of unsteady flows or configurations, J. Fluid Mech. **54**, 143 (1972).

[2] K. Souhar and S. Aniss, Effect of phase thermal modulation without stationary temperature gradient on the threshold of convection, J. Heat Transfer. **138**, 102502 (2016).

[3] A. C. Or and R. E. Kelly, Time-modulated convection with zero mean temperature gradient, Phys. Rev. E **60**, 1741 (1999).

[4] R. G. Finucane and R. E. Kelly, Onset of instability in a fluid layer heated sinusoidally from bellow, Int. J. Heat Mass Transf. **19**, 71 (1976).

[5] T. W. Christopher, M. Le Bars, and S. S. G. Llewellyn, Linear and nonlinear stability of Rayleigh-Bénard convection with zero-mean modulated heat flux, J. Fluid Mech. **961**, A1 (2023).

[6] M. Riahi, M. Hayani Choujaa, S. Er Rajy, and S. Aniss, Primary bifurcation mechanism, heat transfer and bicriticality in time temperature-modulated Rayleigh–Bénard convection in a Hele–Shaw cell, Int. J. Heat Mass Transf. **223**, 125264 (2024).

[7] M. Riahi, M. Hayani Choujaa, and S. Wang, Flow reversal and Neimark-Sacker bifurcations in zero-mean time-modulated temperatures in a Hele-Shaw cell: Floquet theory and Wentzel-Kramers-Brillouin analysis, Int. Commun. Heat Mass Transf. **169**, 109507 (2025).

[8] J. M. Lopez and F. Marques, Modulated Taylor-Couette flow: Onset of spiral modes, Theor. Comput. Fluid Dyn. **16**, 59 (2002).

[9] M. Avila, M. J. Belisle, J. M. Lopez, F. Marques, and W. S. Saric, Mode competition in modulated Taylor-Couette flow, J. Fluid Mech. **601**, 381 (2008).

[10] M. Hayani Choujaa, M. Riahi, and S. Aniss, Inertio-elastic parametric resonance in viscoelastic time-modulated Taylor-Couette flow with zero-mean counter-rotation, Nonlin. Dyn. **114**, 15 (2026).

[11] A. Aouidef, C. Normand, A. Stegner, and J. E. Wesfreid, Centrifugal instability of pulsed flow, Phys. Fluids **6**, 3665 (1994).

[12] F. Marques, J. M. Lopez, and H. M. Blackburn, Bifurcations in systems with $Z_2$ spatio-temporal and $O(2)$ spatial symmetry, Physica D **189**, 247 (2004).

[13] A. Aouidef, C. Normand, and J. E. Wesfreid, Coriolis instability of pulsed flow, Phys. Fluids **7**, 2230 (1995).

[14] W. Chen and C. F. Chen, Effect of gravity modulation on the stability of convection in a vertical slot, J. Fluid Mech. **395**, 327 (1999).

[15] S. Aniss, M. Belhaq, M. Souhar, and M. G. Velarde, Asymptotic study of Rayleigh-Bénard convection under time periodic heating in Hele–Shaw cell, Phys. Scr. **71**, 395 (2005).

[16] G. Seminara and P. Hall, Centrifugal instability of a Stokes layer: Linear theory, Proc. R. Soc. London, Ser. A **350**, 299 (1976).

[17] M. Riahi, S. Aniss, M. Ouazzani Touhami, and S. Skali Lami, Stability of a pulsed Taylor Couette flow in a viscoelastic fluid, J. Soc. Rheol. Jpn. **42**, 321 (2015).

[18] F. Marques and J. M. Lopez, Spatial and temporal resonances in a periodically forced hydrodynamic system, Physica D **136**, 340 (2000).

[19] Y. Bengana, J.-Ch. Loiseau, J.-Ch. Robinet, and L. S. Tuckerman, Bifurcation analysis and frequency prediction in shear-driven cavity flow, J. Fluid Mech. **875**, 725 (2019).

[20] M. Riahi, M. Ouazzani Touhami, and S. Aniss, Reversing and non-reversing Taylor vortex flows in modulated Taylor-Couette flow with counter-oscillating cylinders, Eur. J. Mech. B **95**, 148 (2022).

[21] M. Hayani Choujaa, S. Aniss, M. Ouazzani Touhami, J. Khalid Naciri, and M. Riahi, Stability of an oscillatory Taylor-Couette flow in an upper convected Maxwell fluid, Phys. Fluids **33**, 074105 (2021).

[22] M. Riahi, S. Aniss, M. Ouazzani Touhami, and S. Skali Lami, Centrifugal instability of pulsed Taylor-Couette flow in a Maxwell fluid, Eur. Phys. J. E **39**, 82 (2016).

[23] M. Riahi, S. Aniss, and M. Ouazzani Touhami, Families of reversing and non-reversing Taylor vortex flows between two cooscillating cylinders with different amplitudes, Phys. Fluids **31**, 014101 (2019).

[24] P. Ern and J. E. Wesfreid, Flow between time-periodically co-rotating cylinders, J. Fluid Mech. **397**, 73 (1999).

[25] A. J. Youd, A. P. Willis and C. F. Barenghi, Reversing and non-reversing modulated Taylor-Couette flow, J. Fluid Mech. **487**, 367 (2003).

[26] M. J. Vogel, A. H. Hirsa, and J. M. Lopez, Spatio-temporal dynamics of a periodically driven cavity flow, J. Fluid Mech. **478**, 197 (2003).

[27] J. M. Lopez and F. Marques, Quasiperiodic response to parametric excitations, in *Numerical Methods for Bifurcation Problems and Large Scale Dynamical Systems, IMA Volumes in Mathematics and its Applications*, edited by L. Tuckerman and E. Doedel (Springer, Berlin, 1999), Vol. 119, pp. 209–228.

[28] G. J. Sheard, M. J. Fitzgerald, and K. Ryan, Cylinders with square cross section: Wake instabilities with incidence angle variation, J. Fluid Mech. **630**, 43 (2009).

[29] H. M. Blackburn and G. J. Sheard, On quasiperiodic and subharmonic Floquet wake in stabilities, Phys. Fluids **22**, 031701 (2010).

[30] G. Terrones and C. F. Chen, Convective stability of gravity-modulated double cross-diffusive fluid layers, J. Fluid Mech. **255**, 301 (1993).